

Final Report

ESA STUDY CONTRACT REPORT		
No ESA Study Contract Report will be accepted unless this sheet is inserted at the beginning of each volume of the Report.		
ESA Contract No: 4000130723/20/I-NS	SUBJECT: SSIC-TEAM: A Swarm, SuperDARN, and ICEBEAR Collaboration – Turbulent E-region Aurora Measurements	CONTRACTOR: University of Saskatchewan
* ESA CR()No:	No. of Volumes: 1 This is Volume No: 1	CONTRACTOR'S REFERENCE: UnivRS PAPL 101933
<p>ABSTRACT: The proposed research aimed to investigate plasma density turbulence in the terrestrial auroral ionosphere generated by the Farley-Buneman instability (FBI) using the Swarm satellites and ground based coherent scatter radars. The Swarm satellites are part of the European Space Agency (ESA) Earth Explorers mission, and the Canadian e-POP mission, now known as Swarm-E, was recently added to the Swarm mission as an ESA Third Party Mission. The coherent scatter radars used in the studies include the Ionospheric Continuous-wave E-region Bistatic Experimental Auroral Radar (ICEBEAR) and the Saskatoon Super Dual Auroral Radar Network (SuperDARN) radar. The work corresponds to the priority area of Challenge G5: Different components of the Earth magnetic field and their relation to the dynamics of the charged particles in the outer atmosphere and ionosphere for space weather research, with a focus on Programmatic Area B: Advancing Earth System Science.</p> <p>The Living Planet Fellowship start date was May 2, 2020, with a contract termination date of May 26, 2021. The contract termination was initiated by the postdoctoral fellow due to the acceptance of a long term researcher position with UiT The Arctic University of Norway. Due to this the attached report only covers the first year of the fellowship, and serves as both the Mid-Term Report and the Final Report, as discussed in the Mid-Term Review meeting.</p> <p>The goal of the project was to investigate four different science questions using four unique studies. The four science questions to be investigated were: SQ1. How do the occurrence, amplitude, and velocity of FBI generated plasma density irregularities vary with altitude in the auroral E-region ionosphere? SQ2. Do ionospheric ion upflow velocities and fluxes differ between regions of E-region plasma turbulence and regions of charged particle precipitation? SQ3. Can a measure of E-region plasma turbulence be used as a predictor of the velocity and/or flux of ion upflows? SQ4. Do Alfvén waves modulate the growth rate and phase speed of ionospheric plasma density irregularities generated by the FBI?</p> <p>Using the high temporal and spatial resolution of the Swarm and coherent scatter radar measurements, four studies were proposed to investigate the science questions. This included the development of software to analyze the data from the different instruments. The proposed studies were: SQ1.1: Study 1 – Location and characteristics of ionospheric scatter in relation to aurora SQ1.2: Study 2 – The ionospheric electric field and its relation to ionospheric scatter SQ2 & SQ3: Study 3 – Ion upflow in regions of E-region plasma turbulence SQ4: Study 4 – Evidence of Alfvén waves in Swarm electric fields and E-region ionospheric scatter</p> <p>Software was developed to map the data from the different data sets to a common coordinate system. This included data from the Swarm-E Fast Auroral Imager (FAI) for study 1, where auroral emissions in the near infrared measured by the instrument were mapped to an altitude above the surface of the Earth. Corrections to the mapping had to be performed due to movement of city lights during satellite passes when mapped to the terrestrial surface. A manuscript detailing the mapping of ICEBEAR coherent scatter data was accepted into the journal, Radio Science. Software for mapping and visualization of SuperDARN data was also contributed to. Software for reading in and finding accurate conjunction times for the Swarm A, B, and C, satellite data with the coherent scatter radars was developed. The software is to be posted to a public repository with the submission of a manuscript for study 1 to a scientific journal.</p> <p>Lists of potential conjunctions were created for comparisons between Swarm-E FAI and ICEBEAR, and Swarm A, B, and C and ICEBEAR. SuperDARN was also considered in the analysis, though due to ICEBEAR operating at 49.5 MHz and SuperDARN operating at 8-20 MHz, SuperDARN did not often measure coherent scatter in the same region as ICEBEAR due to significant refraction of the SuperDARN signal by the ionosphere. Conjunctions between ICEBEAR and Swarm were therefore prioritized.</p>		

From the potential Swarm-E FAI and ICEBEAR conjunctions, 3 passes were selected for further analysis. The properties of the E-region coherent scatter measured by ICEBEAR were compared with the brightness of the near infrared auroral emissions measured by the Swarm-E FAI. The near infrared emissions correspond to molecular emission sources in the E-region ionosphere. It was found that the E-region coherent scatter occurred in a specific range of brightness values, and did not occur outside this range. In the bright auroral emission regions there is an enhanced conductance in the E-region ionosphere from the energetic particle precipitation, causing electric fields to be suppressed. The FBI and associated plasma density turbulence require strong electric fields for positive growth, and therefore the suppressed electric field results in a lack of plasma density turbulence for the coherent scatter radar signal to scatter from. In the darker auroral emission regions there is a lack of plasma density to allow for sufficient plasma density irregularity size, resulting in a smaller bulk scattering cross-section for the coherent scatter radar signal. In the comparison between ICEBEAR and Swarm-E FAI data darker regions did correspond to weaker measured coherent scatter signal. The manuscript detailing these results is currently in preparation.

Software for analysis and lists of conjunctions for the remaining studies were developed. Studies 2, 3, and 4 were not further investigated though due to a lack of time and the early termination of the contract.

The work described in this report was done under ESA Contract. Responsibility for the contents resides in the author or organisation that prepared it.

Names of authors: Devin Huyghebaert

** NAME OF ESA STUDY MANAGER:

Roger Haagmans

DIV: Mission Science Division

DIRECTORATE: EOP

** ESA BUDGET HEADING:

- * Sections to be completed by ESA
- ** Information to be provided by ESA Study Manager

FINAL REPORT

A Swarm, SuperDARN, and ICEBEAR Collaboration - Turbulent E-region Aurora Measurements, SSIC-TEAM

Dr. Devin Huyghebaert

University of Saskatchewan

Prepared by
Approved by
Reference
Date of Issue

Dr. Devin Huyghebaert
Dr. Kathryn McWilliams
FR_SSIC-TEAM, UnivRS PAPL 101933
2021-05-14

1 Executive Summary

The Swarm, SuperDARN, and ICEBEAR Collaboration - Turbulent E-region Aurora Measurements (SSIC-TEAM) Living Planet Fellowship project commenced on May 2, 2020, and its goal was to study plasma turbulence in the E-region ionosphere through the use of coherent scatter radars and instruments on board the Swarm satellites. Due to the termination of the contract on May 26, 2021, this Final Report covers approximately a year of work on the SSIC-TEAM project. The contract termination was initiated by the postdoctoral fellow due to the acceptance of a researcher position with UiT The Arctic University of Norway. As only a time of approximately a year is covered, this report serves as both the Mid-Term report and the Final Report, as discussed at the Mid-Term Review Meeting held online on April 28, 2021.

The project proposed to study four different science questions regarding the Farley-Buneman plasma instability and the associated ionospheric phenomena surrounding it. These science questions included how the characteristics of plasma density irregularities associated with the instability vary with altitude, how regions of plasma density turbulence correspond to regions of ion upflow, and if a signature of F-region ionospheric waves were present in E-region plasma density turbulence/irregularities. Four studies were proposed to investigate these questions using the Swarm satellites and ionospheric coherent scatter radar measurements from SuperDARN and ICEBEAR. The four studies involved comparing Swarm-E Fast Auroral Imager (FAI) measurements with E-region coherent scatter, and comparing Swarm A,B,C Electric Field Instrument (EFI) and magnetometer measurements with E-region coherent scatter.

To compare the measurements, software was required to be written for mapping the data from the different instruments to a common coordinate system. The software will be posted with submission of the first manuscript corresponding to the first study proposed, **Study 1** - Location and Characteristics of Ionospheric Scatter in Relation to Aurora. This manuscript was proposed to be submitted to a journal at T0+6, which is 6 months after the start date of the fellowship. The delay was related to an issue found with the Swarm-E FAI mapping, where when data was mapped to the surface of the Earth city lights in the field-of-view (FOV) would move during the satellite pass. As the city lights should be stationary, this then resulted into an investigation into why the movement was occurring. A change to the mapping algorithm was implemented using an ellipsoid Earth model, as well as a slight correction to the FAI pointing direction. The changes reduced the movement of the city lights when mapped to the surface of the Earth, allowing the data to be compared with the coherent radar scatter. The analysis of 3 conjunctions between the FAI and ICEBEAR radar showed that E-region coherent scatter has a range of near infrared auroral emission brightness values that it is coincident with. In the brighter regions there is a lack of coherent scatter due to suppressed/shorted electric fields from enhanced ionospheric conductance, and in the darker regions there is insufficient plasma density for a large enough bulk scattering cross section for coherent scatter to be measured. The manuscript detailing these results is currently in preparation.

The other three studies, **Study 2** - The Ionospheric Electric Field and Its Relation to Ionospheric Scatter, **Study 3** - Ion Upflow in Regions of E-region Plasma Turbulence, and **Study 4** - Evidence of Alfvén Waves in Swarm Electric Fields and E-region Ionospheric Scatter, were not completed during the one year time period. These studies

correspond to comparing measurements from the Swarm A, B, and C satellites and E-region ionospheric coherent scatter. Potential conjunctions between the Swarm satellite and the ICEBEAR coherent scatter radar were found, and software was written to further analyze the conjunctions. The software to map Swarm A, B, and C, orbits to the E-region will be posted with the mapping software relating to Study 1, though further analysis is not planned due to a lack of time.

The SSIC-TEAM proposal discussed comparing the altitude of E-region coherent scatter with the Swarm satellite measurements. Due to unforeseen altitude calibration issues with the ICEBEAR radar, the altitude measurements are only recently becoming available. Ionized meteor trails are being used to calibrate the measurements and a preliminary analysis of the validity of the altitude determination algorithms is underway. For the mapping presented in this report the E-region coherent scatter is mapped to an altitude of 110 km because of this.

Along with the software development and analysis for the comparison of Swarm and coherent scatter radar data, multiple conferences were presented at and attended, a manuscript was published in Radio Science, and a published software package was contributed to. The conferences attended include the EGU General Assembly, the AGU Fall Meeting, and the SuperDARN annual workshop. The manuscript that was published describes mapping the ICEBEAR E-region coherent scatter to the FOV accurately. The software package that was contributed to is for the mapping and visualization of SuperDARN coherent scatter and is named pyDARN.

In summary, the timeline of the SSIC-TEAM project is slightly delayed from what was proposed. Study 1 will be completed, but the analysis for Study 2 is left for a future project. Studies 3 and 4 were proposed for the second year of the project, and since the contract termination is at the approximately 1 year date, these are left for future research. A more detailed breakdown of the background and the work performed in the first year of the fellowship is provided in the following sections.

2 Objectives and Workplan

In the SSIC-TEAM proposal four different science questions were to be investigated over the course of the project. These questions were:

SQ1. How do the occurrence, amplitude, and velocity of FBI generated plasma density irregularities vary with altitude in the auroral E-region ionosphere?

SQ2. Do ionospheric ion upflow velocities and fluxes differ between regions of E-region plasma turbulence and regions of charged particle precipitation?

SQ3. Can a measure of E-region plasma turbulence be used as a predictor of the velocity and/or flux of ion upflows?

SQ4. Do Alfvén waves modulate the growth rate and phase speed of ionospheric plasma density irregularities generated by the FBI?

Four unique studies were proposed to investigate these science questions. In the following list of studies, T0 corresponds to the start of the fellowship, while the number added corresponds to the number of months past this start date. The start date of the SSIC-TEAM project was May 2, 2020. The proposed studies were:

SQ1.1: Study 1 - Location and Characteristics of Ionospheric Scatter in Relation to Aurora (T0+6)

SQ1.2: Study 2 - The Ionospheric Electric Field and Its Relation to Ionospheric Scatter (T0+12)

SQ2 & SQ3: Study 3 - Ion Upflow in Regions of E-region Plasma Turbulence (T0+18)

SQ4: Study 4 - Evidence of Alfvén Waves in Swarm Electric Fields and E-region Ionospheric Scatter (T0+24)

A more detailed schedule for the SSIC-TEAM Living Planet Fellowship schedule is provided in Table 1. SQ1.1: Study 1 involves the use of ICEBEAR, SuperDARN and the Swarm E Fast Auroral Imager (FAI) to investigate the location of coherent scatter with respect to auroral emissions. A manuscript was scheduled to be submitted at T0+6, referring to 6 months after the start of the fellowship. Due to possible issues with mapping the Swarm E FAI to the Earth this has been delayed, though the manuscript is nearing completion. Investigations into SQ1.2: Study 2 have also been commenced, though the results are in a preliminary state and require further analysis.

The software for the analysis and comparison of the Swarm, ICEBEAR, and SuperDARN data sets is operational and will be released shortly, coincident with the submission of the SQ1.1: Study 1 manuscript for publication. This software accurately processes and maps the different data sets to a common coordinate system for comparison. A more detailed description of the software and analysis performed is provided in Section 3.2. A

1 st Kick-off meeting – Teleconference	May 2020 (T0)
Bi-monthly Progress Reports	T0 + 2, 4, 6, etc.
Technical Note 1	T0 + 6
Swarm-E FAI, SuperDARN, ICEBEAR Publication	T0 + 6
AGU Fall Meeting	T0 + 9
Midterm Report	T0 + 12
Midterm Meeting online	T0 + 12
Swarm E-fields, SuperDARN, ICEBEAR Publication	T0 + 12
EGU General Assembly	T0 + 14
Swarm Ion Upflow, SuperDARN, ICEBEAR Publication	T0 + 18
Technical Note 2	T0 + 18
Swarm, SuperDARN, ICEBEAR Alfvén waves Publication	T0 + 24
Final Report	T0 + 24
Final Meeting at ESRIN	T0 + 24 (May 2022)

Table 1: Planned Schedule for the SSIC-TEAM Living Planet Fellowship from the project proposal. The items highlighted in green are projects that are on schedule and/or completed, the items highlighted in yellow are projects that are underway but delayed, and the items not highlighted have yet to be commenced.

general overview of the scientific context of the studies follows below.

3 Work Performed

3.1 Scientific Context

The research related to the SSIC-TEAM project focuses on the Farley-Buneman instability (FBI) [Buneman, 1963; Farley, 1963], also known as the two-stream instability. The FBI is a plasma density instability that has a positive growth rate when electrons in the plasma have a velocity that is greater than the ion velocity by at least the ion-acoustic speed (C_s) [Kelley, 2009]. This instability is able to occur in the E-region of the ionosphere, primarily at altitudes of 90-120 km (C_s is ≈ 400 m/s at E-region altitudes). The instability generates plasma density irregularities at a multitude of characteristic wavelengths, where the growth rate and phase speed of the irregularities are related to the electron motion ($E \times B$ drift) direction [Kelley, 2009]. Information about the FBI can be inferred from measurements of ionospheric plasma density irregularities.

Relating to SQ1, the altitude at which the FBI occurs is important to determining the extent of the turbulence occurring in the E- region ionosphere. By understanding the relationship between the altitude, the electric field, and the growth rate of the FBI it will be possible to better model and predict the physical properties of the ionosphere that are influenced by this instability.

Much of the research surrounding E-region coherent scatter involves the derivation of the background electric fields from the observed radar spectra. An example of a study that accomplishes this is Hysell et al. [2012], where the authors compared VHF E-region coherent scatter with incoherent scatter radar data to test an empirical formula

for determining the electric field from the E-region coherent scatter. This study showed relatively strong correlation of 0.9 between the electric fields derived in this manner and the electric fields determined from the incoherent scatter radar data. Through the studies in the SSIC-TEAM project the electric fields derived from E-region coherent scatter will be investigated in conjunction with the Swarm satellites.

Another study investigating E-region coherent scatter was performed by Chau & St.-Maurice [2016] with analysis of the data by St.-Maurice & Chau [2016]. The authors attempted to characterize and describe the physical reasons for the different spectral widths and Doppler shifts of E-region coherent scatter. The hypotheses resulting from their studies will be further investigated in the present research, where much of the findings revolved around the altitude of the E-region scatter. The research will expand on the understanding of the FBI through obtaining common volume Swarm electric field and high resolution ionospheric scatter measurements. Using the altitude determination capability of the radars, these studies can provide more details about how the electric field affects the phase speed and growth rate of the FBI at different altitudes corresponding to the different characteristics of E-region ionospheric scatter.

Instruments

Swarm E Fast Auroral Imager

The Swarm E Fast Auroral Imager (FAI) [Cogger et al., 2015] measures photons with wavelengths of 650-1100 nm, where the principal emission species in this range are N_2 , O_2 and N_2^+ . The emissions correspond to the locations of energetic particle precipitation. This makes the Swarm E FAI an ideal instrument to investigate the E-region ionosphere in conjunction with coherent scatter radars. The instrument can make measurements up to twice a second (2 Hz), and can be slewed to an area for an extended measurement period during a satellite pass. This increases the possible conjunction times between other instruments and the Swarm E FAI.

Swarm Electric Field Instrument (EFI) and Magnetometer

Swarm A, B, and C, have instruments that measure both the magnetic and electric vector fields in-situ during the satellite orbits. Each satellite has a 3-axis high resolution magnetometer with a sampling rate of 50 Hz and two thermal ion imagers with sampling rates of 16 Hz that measure low-energy ion distributions in the vertical and horizontal planes [Knudsen et al., 2017]. These instruments are able to provide in-situ derived measurements of electric fields, ion upflows, and field-aligned currents. With a 16 Hz sampling rate and an orbit altitude of 500 km, the spatial resolution of the measurements is ≈ 0.5 km. By mapping the data along the magnetic field lines to the E-region, the satellite measurements can be compared with E-region coherent scatter measurements.

Super Dual Auroral Radar Network (SuperDARN)

SuperDARN [Greenwald et al., 1995; Chisham et al., 2007] has been used extensively in space physics studies for over 30 years, and recently some of the radars have been updated with modern software defined radio hardware. The modern digital radio hardware allows the system to run modes that provide enhanced temporal and spatial details of the coherent scatter, which was not feasible with the previous analog system. Borealis Su-

perDARN systems have been installed at many SuperDARN Canada sites, and are being installed at the sites of international SuperDARN partners as well. SuperDARN radars operate in the frequency band of 8-20 MHz, corresponding to plasma density irregularity wavelengths of 7.5-18.8 m, with the SuperDARN Saskatoon radar sharing much of its field of view with ICEBEAR. Previous research has shown that SuperDARN measures both E-region and F-region plasma density irregularities [Greenwald et al., 1995], and it is now possible to implement special modes with the modern SuperDARN Borealis system to obtain temporal and spatial resolutions that are comparable to the ICEBEAR system. Currently investigations are underway to increase the resolution of the SuperDARN radars through simultaneous multi-frequency sounding, full field-of-view imaging, and bistatic operations. This then increases the number of potential conjunction studies, as well as the accuracy, of comparisons between Swarm and SuperDARN measurements.

ICEBEAR

The Ionospheric Continuous-wave E-region Bistatic Experimental Auroral Radar (ICEBEAR) [Huyghebaert et al., 2019] is a 50 MHz VHF ionospheric coherent scatter radar with a $600 \text{ km} \times 600 \text{ km}$ field of view over the auroral zone in Saskatchewan, Canada. ICEBEAR is capable of making full field of view images of E-region plasma density irregularities with wavelengths of $\approx 3 \text{ m}$ every 100 ms (1 s with common mode processing) and with a range resolution of 1.5 km. Using multiple antennas and interferometry techniques, it is possible to determine the angle of arrival of the incoming ionospheric scatter signal. The ICEBEAR receiver array was re-arranged in July, 2019, to provide azimuthal and elevation angle of arrival data. This allows the source of the ionospheric scatter signal to be mapped to 3-D space. This 3-D mapping is currently being investigated, with unexpected behaviour in the determined elevation angles found. These investigations include using meteors to calibrate the elevation angles of the measurements. ICEBEAR has received funding to operate every evening from 0–14 UT, where before operations were on a campaign mode basis. The increase in operations will increase the likelihood of similar location measurements with Swarm.

3.1.1 Study 1

Scientists and researchers have long been fascinated with auroral emissions and the phenomena surrounding them. Through the use of ground based optical measurements and coherent scatter radars the auroral emissions have been investigated with regards to coherent scatter at both F- and E-region altitudes in the past. For F-region studies HF frequency coherent scatter radars with red-line auroral emissions were compared. This provides only an approximate comparison between the data sets, as the altitude range for red-line emissions is typically from 170-230 km [e.g., Megan Gillies et al., 2017], and HF radar signals undergo significant refraction from the ionosphere, especially during geomagnetically active periods. With these resolution considerations in mind, some examples of studies comparing the red-line emission with HF coherent scatter include Milan et al. [1997]; Moen et al. [2001]; Lester et al. [2001]; Chen et al. [2015]. These studies used SuperDARN HF radars to compare the 630 nm auroral emission with characteristics of HF ionospheric coherent scatter.

There have also been studies comparing E-region HF coherent scatter with white light auroral emissions, an example being Hosokawa et al. [2010]. This study showed that the ionospheric coherent scatter occurred between bright regions of auroral emissions, with the conclusion that the electric fields were suppressed in regions of enhanced charged particle precipitation due to the increased conductance from the increase in plasma density. Without a sufficiently large electric field plasma instabilities do not have a large growth rate and plasma density turbulence is not present. This then results in a lack of plasma density irregularities for the coherent radar signal to scatter from.

Comparisons between VHF E-region coherent scatter and green-line emissions have been performed in the past. The benefit of using VHF coherent scatter radars is that there is less refraction in the radar signal, allowing for more accurate spatial determination of the scattering region. Some examples of these types of studies include Bahcivan et al. [2006]; Hysell et al. [2012]. Both these studies showed that often the E-region coherent scatter occurs in regions next to intense auroral emissions. The green-line emissions in the Hysell et al. [2012] study were mapped to 110 km altitude to match the E-region coherent scatter measurements, where the emissions typically peak at ~ 100 km [e.g., Lee et al., 2017].

In addition to coherent scatter studies, there have been comparisons between incoherent scatter radar measurements and auroral emissions. An example of this is provided in Semeter et al. [2009]. In the study it was shown how the white light auroral emissions correspond with incoherent scatter radar measurements from the Poker Flat Incoherent Scatter Radar (PFISR). The results agreed with what was expected, with regions of intense auroral emissions corresponding to regions of enhanced plasma density in the E-region ionosphere.

There have also been satellite measurements of auroral emissions, though rarely are they compared with coherent scatter radar measurements. This could be due to many different reasons, including the resolution of the instruments and the infrequent conjunction times between ground and satellite based instruments. Study 1 of the SSIC-TEAM project looks to further study the relationship between space-borne remote measurements of auroral emissions and E-region coherent scatter.

The idea of an imager to measure auroral emissions on board a satellite has been a longstanding one. For a review of some of the different instruments and satellite missions from the past, the reader is referred to Paxton & Meng [1999]. The review contains information about flown and planned missions spanning 1980-2010.

More recent satellite-borne imager missions and studies include the multi-spectral imager onboard the Japanese Reimei satellite [Obuchi et al., 2008], the optical spectrograph and infrared imager system (OSIRIS) instrument onboard the Odin spacecraft measuring the aurora spectra at 275–815 nm wavelengths from the limb [Gattinger et al., 2010], and the Fast Auroral Imager (FAI) instrument on board the Swarm-E, or e-POP, satellite used in this study [Cogger et al., 2015]. From the Gattinger et al. [2010] study it is important to note that some emissions measured from space have a much different intensity compared to those measured by ground based imagers. One example is the O_2 762 nm emission, where this emission is not seen in ground emissions, but from space based imagers it is significantly greater in intensity.

3.1.2 Studies 2, 3, and 4

For studies 2, 3, and 4, the data from ICEBEAR, SuperDARN, and the Swarm EFI provide an excellent opportunity to investigate small scale structure in the E-region ionosphere. Mapping the data from Swarm down to E-region altitudes along the magnetic field lines to compare with E-region coherent scatter makes it possible to investigate how E-region plasma density turbulence is related to the background electric fields and field-aligned currents. This includes comparing characteristics of E-region coherent scatter with the ionospheric electric fields in the region [e.g., Hysell et al., 2012], comparing ion upflow regions with regions of ionospheric plasma density turbulence [e.g., Wahlund et al., 1992], and comparing spectral analyses of coincident Swarm and ICEBEAR measurements to investigate ionospheric wave-like structures. Due to limited time, studies 2, 3, and 4 were not thoroughly investigated.

3.2 Methods

3.2.1 Mapping Swarm A, B, C Data

Software has been written to read in the Swarm data files available at <https://swarm-diss.eo.esa.int/> and plot the measurements to a map with geographic latitude and longitude coordinates. Currently the routines support reading in data files of the following types: Level 2 daily FAC, 16 Hz EFI faceplate plasma density, 16 Hz EFI cross track velocities, 50 Hz high resolution magnetometer, and 2 Hz Langmuir probe measurements. Based on the latitude and longitude bounds set by the user, any satellite orbits that pass through these bounds are determined after reading in the associated data file. The satellite pass is then mapped down the geomagnetic field lines to E-region altitudes (110 km) using the AACGM software library [Burrell et al., 2020; Shepherd, 2014]. The data parameter the user has set to plot will be shown on the map(s) generated as colored measurement points corresponding to the value at each point and with a user set scale. There is also an option to include a line plot of multiple different measurement quantities for the pass.

This setup allows the comparison of data even when measurements are not coincident in time and/or space. The user must be careful when using measurements that are not coincident, and consideration of the effects from these offsets must be included. An example of this software in conjunction with coherent scatter radar data is provided in Section 3.2.5. The software still requires to be tested and verified, though as will be shown, it is at a satisfactory state for preliminary analysis of conjunctions between Swarm and coherent scatter radars.

3.2.2 Mapping Swarm E Data

The basis of the software for mapping Swarm E Fast Auroral Imager (FAI) data to the Earth was obtained from the Swarm E operations team. The FAI pointing direction is based on the Swarm E satellite attitude information provided with the FAI data. Each pixel from the imager is mapped to a circular FOV and a pointing direction is determined for each of these pixels. These pixel pointing directions are then used to map the auroral emission measurements to a map with latitude and longitude coordinates.

With the mapping software provided, city lights would move during the satellite pass when the data was mapped to the surface of the Earth. An investigation into why this was occurring was performed.

As part of the investigation into the Swarm-E Fast Auroral Imager (FAI) mapping software, a new method for determining the latitude and longitude of the emissions was developed. This served to improve the location determination and remove a potential source of mapping error for emission location verification. The algorithm uses an ellipsoid model of the Earth to determine the location where a line originating at the Swarm-E satellite passes into that ellipsoid, with a set altitude above the surface. The equations for the new ellipsoid mapping algorithm are provided below.

$$X = x_0 + x_s t \quad (3.1)$$

$$Y = y_0 + y_s t \quad (3.2)$$

$$Z = z_0 + z_s t \quad (3.3)$$

$$\frac{X^2}{a^2} + \frac{Y^2}{a^2} + \frac{Z^2}{b^2} = 1 \quad (3.4)$$

The variables x_0 , y_0 , and z_0 correspond to the Cartesian coordinates of the satellite in a geocentric coordinate system, x_s , y_s , and z_s correspond to the change in each of the coordinates for an increment in t , and X , Y , and Z correspond to the Cartesian coordinates of the line. The variables a and b correspond to the major and minor axes of an ellipsoid. In the case of the Earth, $a = 6378.1366$ km and $b = 6356.7519$ km. By substituting the Cartesian coordinates X , Y , and Z into equation 3.4, the equation becomes a second order polynomial equation. The value of t can be determined using a quadratic solver, as x_0 , y_0 , z_0 , x_s , y_s , and z_s are known. Solving a quadratic equation typically results in two solutions, where the one that is closer to the satellite is chosen to be the correct mapped location. The solution at a further distance is the point where the line exits the Earth ellipsoid. The Cartesian coordinates of the intersection point are then converted to a latitude, longitude, and altitude (WGS84 format).

The Swarm-E FAI data mapped to the surface of the Earth were again compared with the expected location of terrestrial city lights after the ellipsoid model was implemented. The mapping displayed that there were still some corrections to be made to the mapping algorithm, as the city lights would move during the pass of the satellite, sometimes by as much as 3 degrees in latitude and longitude. The ellipsoid model did provide more accurate mapping of the FAI pixels compared to the previous model, based on the altitudes obtained when converting to WGS84 format.

Through trial and error of slightly changing imager variables, such as the pointing direction and imager viewing area, a correction to the mapping of the imager was found. The correction was determined by shifting the pixels in the imager arrays, effectively steering the imager slightly in the azimuth and elevation directions. A shift of -6 pixels in one direction and 6 pixels in the other direction was found to greatly reduce the movement of city lights measured by the FAI during the satellite pass. This corresponds to angular corrections of $\sim -0.62^\circ$ and 0.62° in the x- and y- directions of the imager.

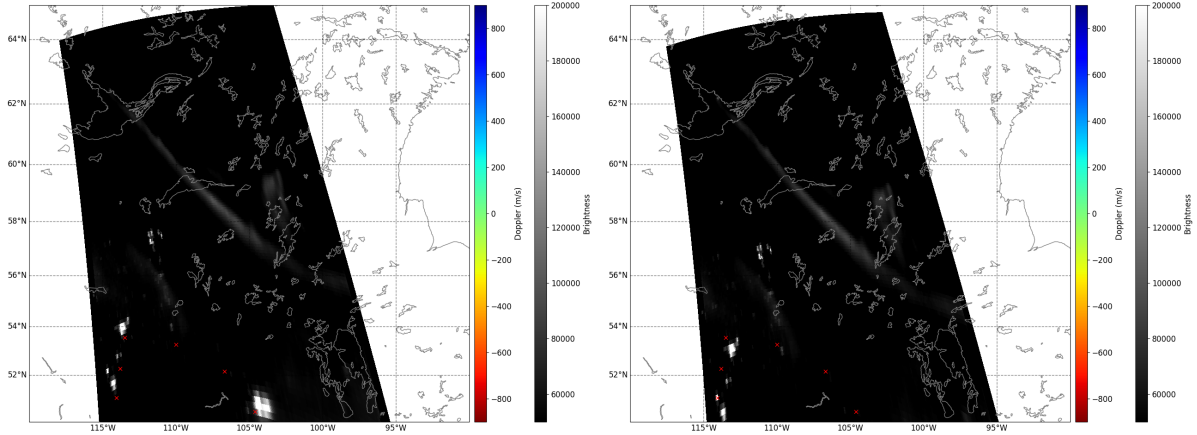


Figure 1: Example of the FAI data mapped to the ground without (left) and with (right) the imager pointing correction of -0.62° in the x-direction (rows on imager) and 0.62° in the y-direction (columns on imager). The red ‘x’ labels in the figure correspond to expected locations of city lights. The fact that the expected location of the city lights are closer to the imager than the data shows could be due to refraction of the city lights by the atmosphere.

An example of the FAI data with and without the pointing direction correction is shown in Figure 1. The left image shows the FAI data without the correction, while the right image shows the data with the correction. The data is mapped to the surface of the Earth for comparison with the expected location of city lights in the field of view. Even with the correction, the city lights are located on the opposite side of the expected city lights location with respect to the Swarm-E satellite. This is attributed to refraction, though further adjustments and improvements to the mapping corrections are possible in the future. With the current implementation the city lights remain in a relatively consistent location across the satellite pass.

3.2.3 Mapping ICEBEAR Data

The ICEBEAR data is mapped to the FOV using a fitting algorithm to the cross-spectra measured between antennas in the radar antenna array. For the work presented here, only the antennas along a single axis are used, also known as a linear array. By fitting a Gaussian to the cross-spectra measured, it is possible to determine the azimuth and azimuthal extent of the incoming coherent radar scatter. This is important as ionospheric coherent scatter is a spread target that can originate from a large portion of the FOV simultaneously. The algorithm for fitting the ICEBEAR cross-spectra has been published in Radio Science [Huyghebaert et al., 2021]. As the fitting process requires a significant amount of computer processing time, the output from the fitting software is saved in HDF5 files to be used for mapping the E-region coherent scatter for future studies. This current method does not obtain elevation angles for altitude determination of the ICEBEAR coherent scatter. Verification and calibration of a method to determine accurate elevation angles is currently underway using meteor echoes.

Once the azimuth and azimuthal extent of the coherent scatter is determined the

data is able to be mapped to the ICEBEAR FOV. Software has been written as part of the SSIC-TEAM project to accurately map the data to the FOV at an altitude of 110 km. This includes the determination of the SNR, doppler shift, and spectral width of the ionospheric scatter spectra. These spectra characteristics are important for understanding the characteristics of the ionosphere required to produce the plasma density irregularities.

To determine the characteristics of the coherent scatter spectra, a Gaussian-like distribution is fit to the spectra for each range-azimuth bin. The azimuth resolution can be set by the user, though 0.5 degrees is currently what is used. The equation that is fit to the spectra is,

$$f(x) = SNR \times \exp\left(\frac{-(x - d)^2}{2\sigma^2}\right). \quad (3.5)$$

SNR is the peak signal to noise ratio, d is the average Doppler shift, σ is the spectral width, and x is the Doppler shift. An example of a fitted spectra is shown in Figure 2. To convert the spectral width value calculated to the Full-Width-Half-Max (FWHM) value, the spectral width can be multiplied by 2.355.

A slight modification was implemented for the fitting algorithm, where if there is a measurement at a Doppler shift anywhere in the FOV at a given range and the SNR is less than 0.75, that bin is set to a value of 0.75 SNR. A value of 0.75 SNR is less than the noise level, but is above the 0 SNR floor for the fitting process. This minimally affects data with a large SNR, but serves to broaden the spectral width of data with a small SNR. From observing and analyzing many different spectra, this adjustment provides an improvement to the fitting method.

3.2.4 SuperDARN Data Visualization and New Operational Capabilities

To read in SuperDARN formatted files pyDARNio [SuperDARN Data Standards Working Group (DSWG) et al., 2020] was used. Software was written to take the data from these files and, assuming straight line propagation, plot the SuperDARN coherent scatter that was likely coming from the E-region. As the SuperDARN radars operate at HF radio frequencies, assuming straight line propagation of the radio wave is not typically a reasonable assumption. Since only coherent scatter originating from lower altitudes was being plotted, which was determined based on the elevation angle determination of the SuperDARN coherent scatter, the assumption of straight line propagation is considered to be reasonable. There could be some offset in the location of the scatter, but this provided an approximation that could be used to map the scatter.

Development has been ongoing on a SuperDARN data visualization software library by the international SuperDARN group. This software is called pyDARN [SuperDARN Data Analysis Working Group (DAWG) et al., 2021], and it was decided to contribute to the development of this library in the hope it could be useful for the SSIC-TEAM project. The location of SuperDARN range gates have since been incorporated into pyDARN by the software development group, and could be incorporated into the SSIC-TEAM analysis software in the future.

Currently the focus of the SSIC-TEAM project has been on comparisons between Swarm and ICEBEAR data. This is due to a lack of SuperDARN coherent scatter measurements in regions of auroral emissions. The reason for this is that the SuperDARN

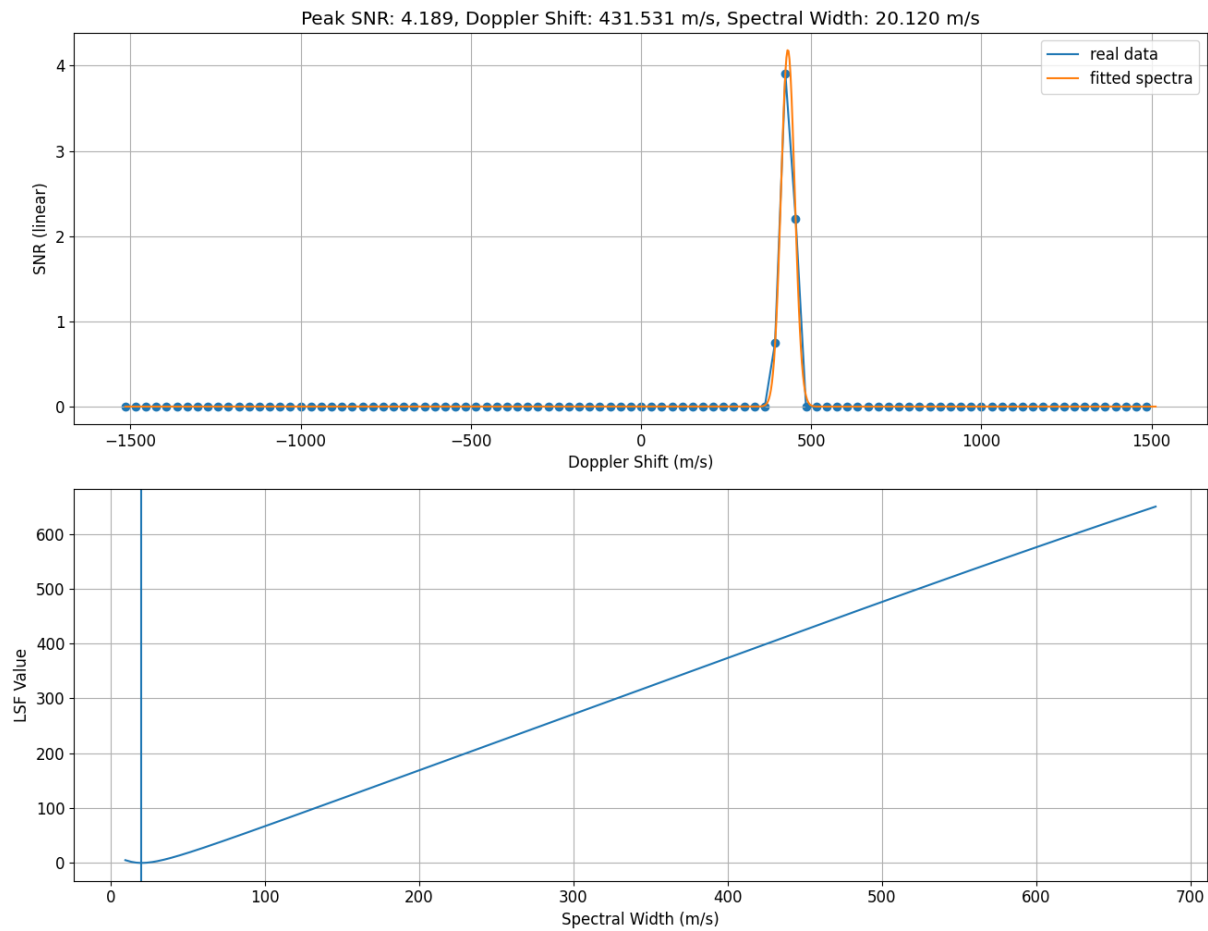


Figure 2: Example for fitting the ICEBEAR spectra to derive the peak SNR, Doppler shift, and the spectral width for a given range and azimuth in the ICEBEAR FOV. The top panel shows the real and fitted data, while the bottom panel is used as a check that the spectral width is fit correctly.

radars operate at HF radio frequencies, while ICEBEAR operates at VHF radio frequencies. The HF signal significantly refracts with a strongly ionized E-region, resulting in the signal not reaching regions for E-region coherent scatter to occur. There is also the matter of the temporal and spatial resolution of SuperDARN being more coarse than that of ICEBEAR and the Swarm satellite measurements.

One way of improving the temporal and spatial resolution of the SuperDARN radars is through the use of new operational capabilities made possible by the modernized SuperDARN Borealis hardware and software upgrade. As part of the SSIC-TEAM project, contributions have been made to implementing new radar modes for this purpose. Pulse phase encoding, simultaneous dual frequency operations, and spread transmitter beam full FOV imaging are all in preliminary testing phases and will eventually be available for future conjunction experiments.

3.2.5 Swarm A,B,C and Coherent Scatter Data Comparisons

To find conjunctions when both Swarm A, B, and C satellite measurements and ICEBEAR data are present, the VirES data visualization portal and ICEBEAR summary plots were used. By comparing times when the Swarm satellites pass through the ICEBEAR FOV with when ICEBEAR measured coherent scatter it was possible to greatly reduce the dates and times to further investigate and analyze. The dates that were selected for further analysis are given later in Section 3.4.2.

Using the software developed to map the SuperDARN and ICEBEAR coherent scatter, and the Swarm satellite paths, the possible conjunctions could be further studied. An example of data from a conjunction is shown in Figure 3. In Figure 3 the top 3 maps are snapshots of the data during the Swarm pass through the ICEBEAR field of view, while the bottom panel provides the data for the full Swarm pass. The SuperDARN, Swarm, and ICEBEAR data are all shown in the maps, with the field aligned current being measured from Swarm. Other parameters measured by Swarm can also be plotted with a simple change to the input arguments for the plotting function. Swarm B is the satellite in this pass and has its data mapped along the magnetic field lines to a 110 km altitude for comparison with the coherent radar scatter.

3.2.6 Swarm-E FAI and ICEBEAR Comparisons

The ICEBEAR and Swarm-E FAI data were mapped to a latitude/longitude terrestrial coordinate system at 110 km altitude. An example of 1 second of data with data from both instruments mapped to the ICEBEAR FOV is shown in Figure 4. SuperDARN is also included in this figure, though it was not further considered in the current analysis. The center of each ICEBEAR range-azimuth bin was determined and the auroral emission brightness value as measured by the FAI corresponding to this point was recorded. This was repeated for each one second measurement during the pass. The result was a data set of E-region scatter and corresponding brightness values for the pass.

Along with the brightness of each pixel, the direction and magnitude of the brightness gradient were investigated. A forward difference method was applied to the array of imager data to obtain two vectors for the change in brightness between points for each pixel location. As these vectors are not necessarily perpendicular once mapped to the

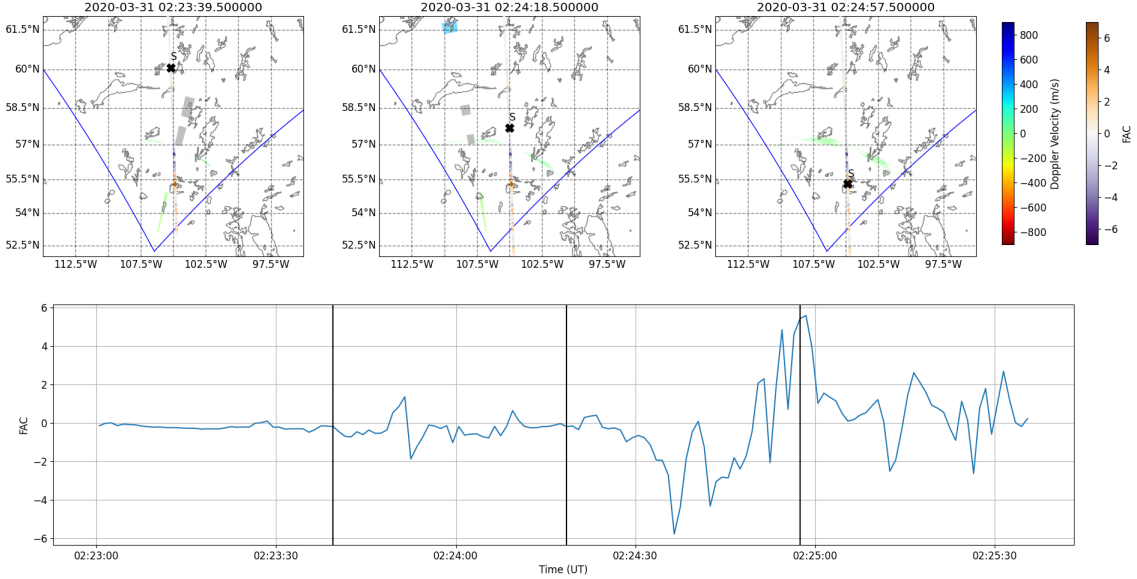


Figure 3: An example of the plotting software developed for the SSIC-TEAM project. SuperDARN, Swarm, and ICEBEAR data are plotted with a common reference frame at 107 km altitude. The data from the full Swarm pass are plotted on the maps, with the location of the satellite for that time shown by the ‘x’.

Earth, a normalization of the vectors was performed to determine perpendicular vectors and add them together. This then provided a 2D vector for a change in brightness per km for each of the FAI pixels. The direction of the gradient was determined with respect to the ICEBEAR radar signal bisector. An example of the brightness gradient is shown in Figure 5. The left plot shows the brightness gradient direction without any smoothing applied to the FAI data. This data was determined to be contaminated with noise, so a Gaussian smoothing method was implemented on the initial brightness values before taking the gradient of the data. The result is shown in the right image of the figure, where it is evident that the noise is sufficiently suppressed.

The magnetic field vector was also determined at the location of the E-region coherent scatter using the IGRF model for 2020 [Alken et al., 2021]. This provided a means by which to calculate the aspect angle of the coherent scatter, which is an important factor for coherent scatter radar studies as the plasma density irregularities are assumed to be approximately aligned along the magnetic field lines. The aspect angle was calculated and recorded along with the E-region coherent scatter and FAI characteristics.

The methods here provide a data set of E-region coherent scatter corresponding to the characteristics of auroral emissions as measured by the Swarm-E FAI. A further analysis of the data is provided in Section 3.4.1.

3.3 Data

ICEBEAR data will be accessible from a data repository in the future. Until the data repository is implemented, ICEBEAR data used in publications will be deposited in the Zenodo data repository. A prototype data repository for ICEBEAR data is becoming

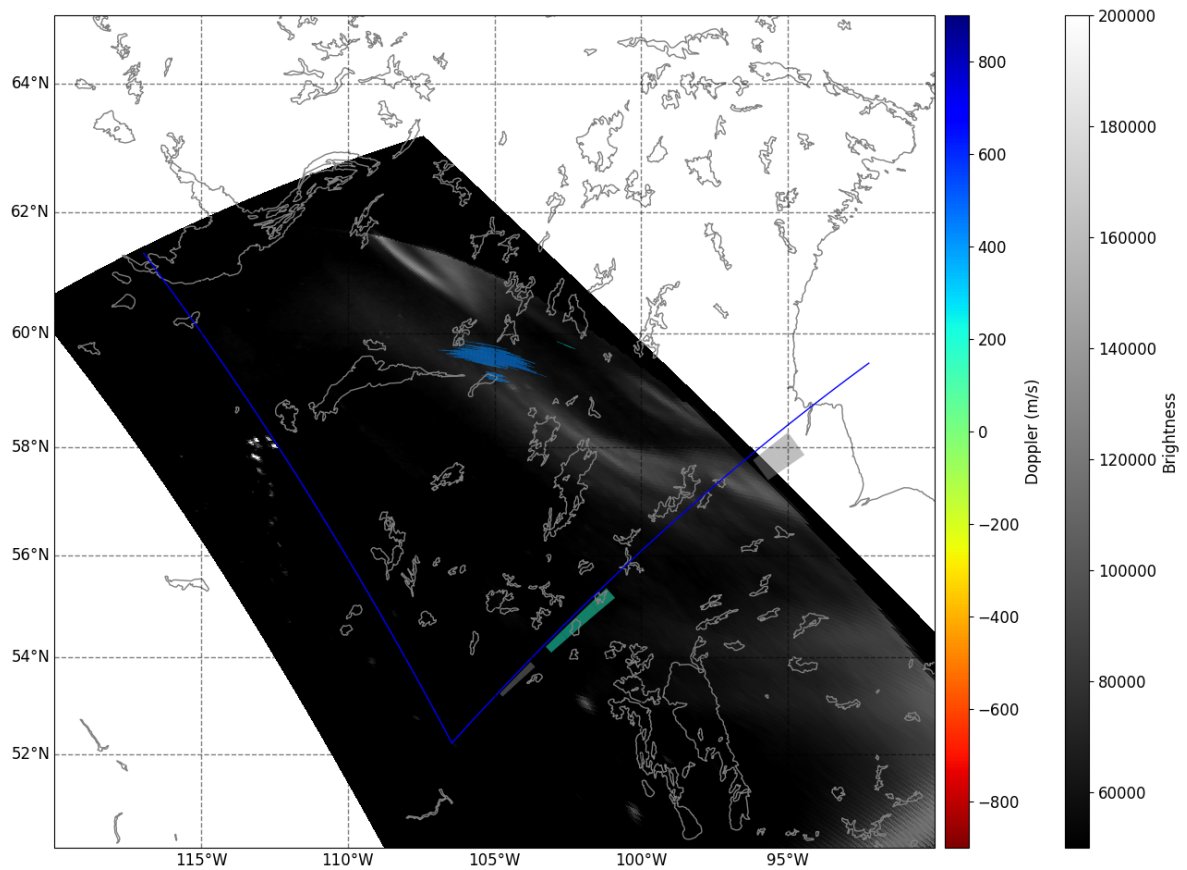


Figure 4: 1 second snapshot of ICEBEAR, SuperDARN and FAI data corresponding to 2018-03-10 05:21:48 UTC. The green and grey boxes are SuperDARN Doppler velocity data, the blue region are ICEBEAR Doppler velocity data, and the grey scale image is the brightness as measured by the FAI.

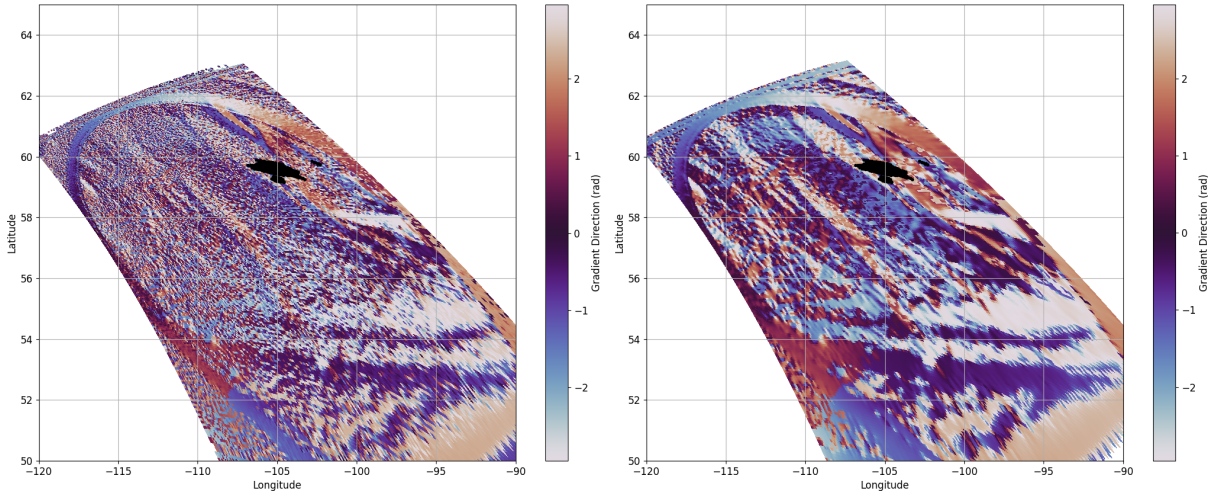


Figure 5: Example of the brightness gradient determination from the FAI instrument. The left plot is without smoothing, while the right plot is with a Gaussian smoothing method to reduce the noise in the FAI measurements before determining the brightness gradient. The black regions correspond to locations where ICEBEAR E-region coherent scatter was measured. The color scale displays how the direction of the brightness gradient corresponds to the ICEBEAR coherent scatter. This is a 1 second measurement taken at 2018-03-10 05:21:48 UTC, corresponding to the same time as Figure 4.

operational and some initial data are accessible at http://ion.usask.ca/data_access/.

A preliminary version of Swarm E FAI data mapped to latitude and longitude in an HDF5 format was acquired upon request from the instrument team. The algorithm to map the imager data produces an image in latitude and longitude coordinates at an altitude of 110 km. The mapping software has been shared and the HDF5 files are able to be generated from the level 0 Swarm E FAI data locally. The level 0 data for Swarm E is accessible at <https://epop-data.phys.ucalgary.ca/>.

SuperDARN Canada provided access to the SuperDARN data. SuperDARN data can be accessed by request through any of the SuperDARN partners.

Swarm A, B, and C data from the magnetometers and EFI instruments are available through the Swarm data portal located at <https://swarm-diss.eo.esa.int/>.

3.4 Results

From the SSIC-TEAM Living Planet Fellowship proposal, four different studies were discussed addressing the science questions of the project. The software for these studies is nearing completion, with analysis for SQ1.1: Study 1 - Location and Characteristics of Ionospheric Scatter in Relation to Aurora already performed. The results of the analysis for these studies is provided below.

3.4.1 Study 1

Conjunctions between ICEBEAR and the Swarm-E FAI were analyzed for use in this study. The green and yellow highlighted conjunctions in Table 2 are times which have

Date	Sat.	Pass Start (UT)	Pass End (UT)
2018-03-10	E	05:21:13	05:27:45
2018-04-11	E	07:41:13	07:46:45
2018-04-13	E	08:33:13	08:40:45
2019-10-25	E	03:25:14	03:31:46
2019-10-27	E	04:02:14	04:18:46
2019-10-27	E	07:27:14	07:41:46
2020-03-19	E	03:45:14	03:56:45
2020-03-19	E	07:15:14	07:26:45
2020-03-19	E	08:57:14	09:10:44
2020-04-15	E	04:34:44	04:42:16
2020-04-15	E	06:16:39	06:25:14
2020-04-18	E	03:09:42	03:13:29
2020-05-06	E	04:40:59	04:45:30
2020-10-24	E	02:36:44	02:38:16
2020-10-26	E	06:32:44	06:45:55

Table 2: Potential Swarm E FAI conjunctions with ICEBEAR. The green highlighted rows are passes that are used in the present study. The yellow highlighted rows are passes that have both FAI and ICEBEAR data, but the FAI pointing direction is near horizontal to the surface of the Earth making it difficult to reliably use the data for comparisons with ICEBEAR.

both E-region coherent scatter measured by ICEBEAR and Swarm-E FAI data. It was found that after the FAI pointing direction corrections were made and the FAI data were mapped to a latitude and longitude coordinate system, some of the passes were near a horizontal viewing position with respect to the surface of the Earth and were not viable for the study. The horizontal viewing angle caused the resolution of the imager when mapped to 110 km altitude to be poor. Three passes were deemed to be viable for the study, and are the green highlighted rows in Table 2.

The three passes highlighted in green in Table 2 were further analyzed using the methods described in Section 3.2. For this report the results from the pass on 2018-03-10 will be shown. The other passes will also be included in the study corresponding to SQ1.1: Study 1 - Location and Characteristics of Ionospheric Scatter in Relation to Aurora for the SSIC-TEAM project when it is submitted for publication to a journal.

Figure 6 shows how the auroral emission brightness measured by the FAI corresponds to the E-region coherent scatter measured by ICEBEAR. As the scatter and emissions are both mapped to 110 km, the aspect angle is only approximate and is expected to change with altitude. From analyzing this plot along with Figure 4, it is clear that the E-region coherent scatter occurs not the brightest auroral NIR emission regions, but also not in the darkest. This finding was consistent across all three passes analyzed, where the E-region coherent scatter occurs in regions of brightness between 25,000 and 125,000.

For E-region coherent scatter to be measurable, two things are required.

1. A sufficiently strong E-field to generate the plasma density irregularities [e.g., Kelley, 2009]

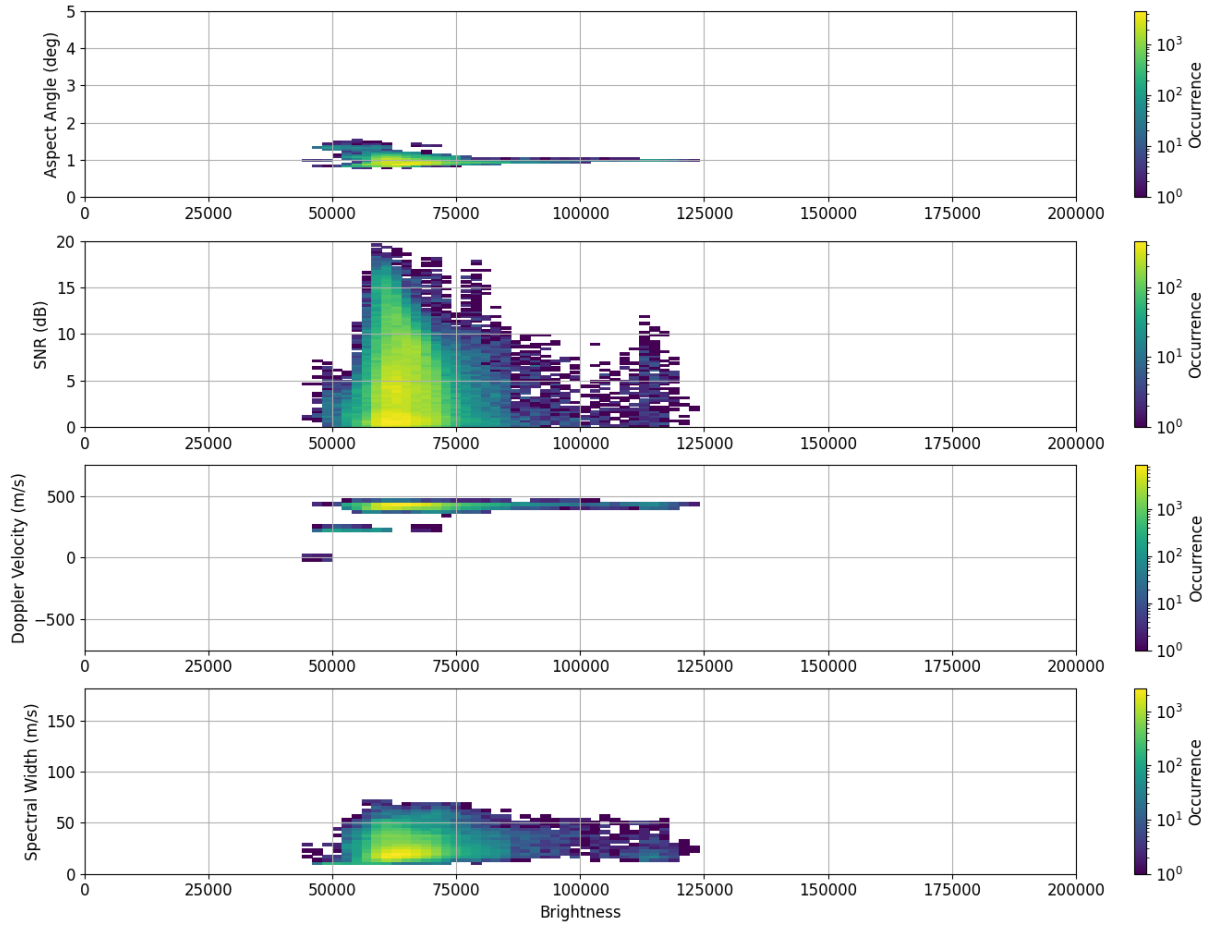


Figure 6: Data from the 2018-03-10 Swarm-E pass listed in Table 2. The brightness as measured by the Swarm-E FAI is on the x-axis, while parameters corresponding to the E-region coherent scatter measured by ICEBEAR are listed on the y-axes. The plots are 2d histograms of the quantities, showing how the brightness corresponds to the difference E-region coherent scatter characteristics.

2. Sufficient electron density for a large bulk scattering cross-section to detect the scattered radar signal [e.g., Hysell, 2018]

The scattering cross section for coherent scatter radar studies is proportional to $(\frac{\Delta N_e(\mathbf{k})}{N_e})^2 N_e^2$ [e.g., Hysell, 2018], where N_e is the electron density and \mathbf{k} is the plasma density irregularity wavenumber. If we assume a consistent ratio of $\frac{\Delta N_e(\mathbf{k})}{N_e}$ for the plasma density irregularities, this results in the scattering cross section being dependent on the electron density. A factor of 10 in electron density therefore changes the SNR by 20 dB. A factor of 10 change in the irregularity size with respect to the background electron density also changes the SNR by 20 dB.

In the darker regions of the FOV, there is insufficient plasma density for measurable scatter due to a lower bulk scattering cross section, even with sufficiently strong electric fields for plasma density irregularity growth. In the very bright regions the electric fields can be suppressed/shorted [e.g., Marklund, 1984], resulting in insufficient conditions for positive growth rates for plasma density irregularities. This is an important consideration for the measurement and understanding of E-region plasma density irregularities, especially with respect to plasma density enhancements caused by particle precipitation in the night time sector.

The brightness gradients were also investigated for the Swarm-E FAI passes in conjunction with ICEBEAR E-region coherent scatter. The results from the pass on 2018-03-10 are shown in Figure 7. The aspect angle of the coherent scatter with the geomagnetic field are on the x-axis and were all found to be greater than 0, meaning that the angle between the coherent scatter radar bisector and the geomagnetic field is greater than 90 degrees. There was minimal dependence on the gradient direction for the location of the E-region coherent scatter, though the other two passes did show a relationship (not shown here). With only 3 passes of data, that relationship was determined to likely be a coincidence due to the small sample size and a more extensive analysis would be required to determine if a relationship truly does exist.

The scale length sizes for both brightness and N_e are found to be quite large, where the scale length refers to the distance required for the quantity to double based on the gradient. These parameters are left for a potential future study and will not be further investigated here. The main finding from this comparison between the Swarm-E FAI and ICEBEAR coherent scatter data is that the E-region coherent scatter is found to fall within a range of brightness values measured by the FAI. The bounds of this brightness range are determined by the electric fields being suppressed due to enhanced conductivity in regions of bright auroral emissions, and having an insufficient bulk scattering cross-section for coherent scatter to be measured in regions with a lack of emissions.

3.4.2 Study 2, 3, & 4

Studies 2, 3, and 4 of the SSIC-TEAM proposal involve the comparison of ICEBEAR and SuperDARN data with measurements from the instruments onboard the Swarm A, B, and C satellites. Potential conjunction candidates for these studies are provided in Table 3. A description of how these dates and times were found was provided in Section 3.2.5. In the table the rows highlighted in green are viable candidates for studies after further investigations of the data, while the rows highlighted in yellow have yet to be investigated.

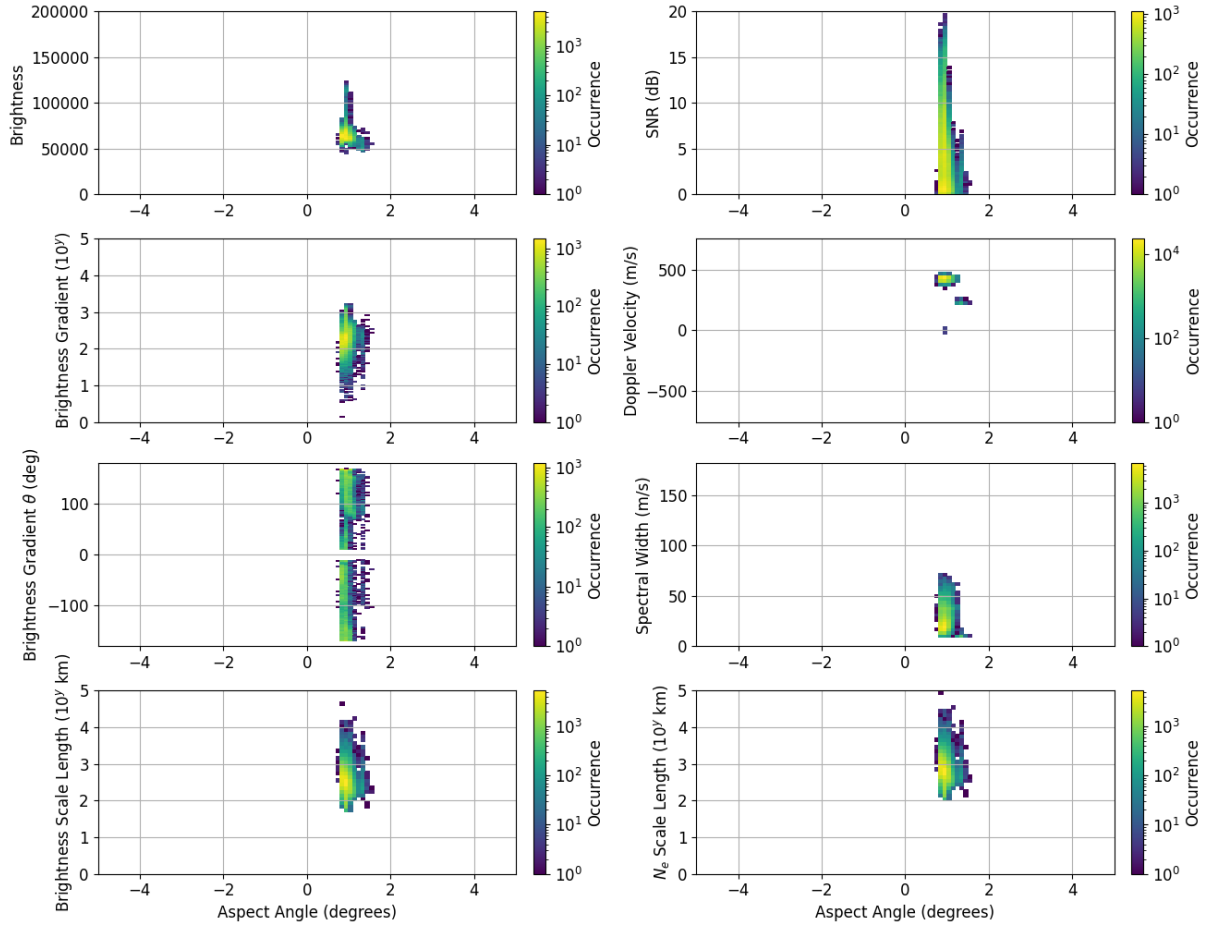


Figure 7: Data from the 2018-03-10 Swarm-E pass highlighted in green in Table 2. The plots shown here compare the aspect angle of the scatter to the many different E-region coherent scatter and Swarm-E FAI measurement properties. The Brightness gradient is calculated with respect to the bisector of the ICEBEAR coherent scatter, and the N_e scale length is calculated considering a relationship of $\text{Brightness} \propto N_e^2$ based on the relationship mentioned in Semeter et al. [2009] for white light auroral emissions.

Date	Sat.	Pass Start (UT)	Pass End (UT)
2018-03-15	C	00:32:00	00:33:15
2018-03-15	A	00:32:00	00:33:15
2018-03-17	C	00:47:19	00:49:00
2018-03-17	A	00:47:19	00:49:00
2018-04-11	B	04:09:12	04:10:30
2018-04-11	A	09:39:50	09:41:00
2018-04-11	C	09:39:50	09:41:00
2019-09-01	A	00:41:00	00:43:00
2019-09-01	C	00:41:00	00:43:00
2019-09-01	C	11:51:00	11:53:00
2019-09-01	A	11:51:00	11:53:00
2019-09-03	B	08:49:30	08:51:30
2019-10-25	B	04:35:00	04:36:15
2019-10-25	C	06:52:45	06:54:00
2019-10-25	A	06:52:45	06:54:00
2020-03-19	A	06:34:05	06:36:00
2020-03-19	C	06:34:05	06:36:00
2020-03-31	B	02:23:30	02:25:30
2020-05-30	A	11:08:36	11:10:30
2020-05-30	C	11:08:36	11:10:30
2020-07-14	B	05:43:25	05:45:25
2020-07-14	C	07:09:15	07:11:15
2020-07-14	A	07:09:15	07:11:15
2020-09-28	B	11:09:29	11:11:30
2020-09-29	B	10:49:00	10:51:00
2020-10-01	B	10:10:27	10:12:30
2020-10-24	B	08:57:15	08:59:15
2020-11-20	B	06:24:10	06:25:20
2020-12-09	B	04:54:00	04:55:20
2020-12-22	B	03:47:10	03:48:20
2021-01-12	B	01:37:00	01:38:10
2021-02-19	B	10:56:43	10:58:00
2021-02-19	A	11:18:01	11:20:00
2021-02-19	C	11:18:01	11:20:00
2021-02-25	B	10:31:00	10:33:00
2021-03-01	A	10:39:00	10:41:00
2021-03-01	C	10:39:00	10:41:00

Table 3: Potential Swarm A, B, and C conjunctions with ICEBEAR. The green highlighted rows are passes that are good candidates for future studies. The yellow highlighted rows are conjunctions that have yet to be analyzed.

One of the interesting questions that arose from a preliminary investigation into the data was if the field-aligned current intensity was a precursor for E-region plasma density irregularities to be present. This could potentially correspond to the results from Study 1, where some charged particle precipitation is required for E-region coherent scatter to be measured. The possible correlation between the FAC intensity data and location of E-region coherent scatter was noticed during the software development for mapping the Swarm and coherent scatter data to a common coordinate system, but has not been investigated in detail.

Investigations into the electric fields, ion upflows, and wave activity measured by Swarm in conjunction with coherent scatter radar measurements have not been investigated, as Study 1 has been focused on. With the conjunction dates determined and the software developed to compare the data sets, the analysis of this data is a great future project.

4 Conclusions and Recommendations

Software for mapping Swarm E FAI, Swarm A, B, and C, SuperDARN and ICEBEAR data has been developed. This software is able to be used to compare the different data sets in a common coordinate system. Some testing and verification is still required for the Swarm A, B, and C algorithms for mapping the satellite track down the geomagnetic field lines to the E-region ionosphere, though initial results are promising. Corrections were made to the Swarm E FAI pointing direction after issues were found with city lights changing location during a satellite pass when the data were mapped to the surface of the Earth. After the corrections the city lights were much more confined in space during the satellite pass. A fitting algorithm was developed for ICEBEAR coherent scatter measurements to properly map the coherent scatter to the radar FOV, which resulted in a publication in the journal *Radio Science*. Using the mapping algorithms developed for the Swarm E FAI and ICEBEAR, Study 1 was able to be investigated.

The manuscript for SQ1.1: Study 1 - Location and Characteristics of Ionospheric Scatter in Relation to Aurora will be completed and submitted relatively soon. The journal that it will be submitted to is either *Geophysical Research Letters* or *JGR: Space Physics*. The visualization and analysis software will be published along with the submission of the manuscript. The main finding from this manuscript includes that E-region coherent scatter radar measurements occur in a range of auroral emission brightness values, but rarely at brightness values outside the range. This is explained due to electric fields being suppressed in regions of intense auroral precipitation and enhanced ionospheric conductance, and the bulk scattering cross section for coherent radar scatter being low in low plasma density regions corresponding to a lack of auroral emissions. For a detailed description of the results, refer to Section 3.4.1.

Funding has been obtained for continuous operation of the ICEBEAR radar, which has occurred since October, 2020. This provides an extended data set for comparison with Swarm satellite passes, especially since active geomagnetic conditions have occurred more frequently lately. Work is still underway to obtain accurate altitude data from the ICEBEAR coherent scatter radar, but progress is being made using ionized meteor trails for calibration.

Swarm-E FAI, SuperDARN, ICEBEAR Publication	T0 + 6
Swarm E-fields, SuperDARN, ICEBEAR Publication	T0 + 12
Bi-monthly Progress Reports	T0 + 14, 16, 18, etc.
Swarm Ion Upflow, SuperDARN, ICEBEAR Publication	T0 + 18
Technical Note 2	T0 + 18
Swarm, SuperDARN, ICEBEAR Alfvén waves Publication	T0 + 24
Final Report	T0 + 24
Final Meeting at ESRIN	T0 + 24 (May 2022)

Table 4: Planned Schedule for Living Planet Fellowship

A list of conjunctions to be used for Studies 2, 3, & 4 are provided in Table 3. These dates can be used to further investigate the relationship between ionospheric coherent scatter and electric fields, ion upflows, and wave-like ionospheric activity.

Due to the termination of the contract, the majority of the second year of work will not be performed. This includes not completing Study 2, 3, & 4 with the current contract. Study 1 and the SSIC-TEAM software will be submitted and published, though potentially after the submission of this report.

Table 4 provides a timeline of the tasks left for the SSIC-TEAM Living Planet Fellowship project, with the rows highlighted in yellow currently underway/delayed.

5 References

- Alken, P., Thébault, E., Beggan, C. D., Amit, H., Aubert, J., Baerenzung, J., ... others (2021). International geomagnetic reference field: the thirteenth generation. *Earth, Planets and Space*, 73(49), 1–25. doi: <https://doi.org/10.1186/s40623-020-01288-x>
- Bahcivan, H., Hysell, D. L., Lummerzheim, D., Larsen, M. F., & Pfaff, R. F. (2006). Observations of colocated optical and radar aurora. *Journal of Geophysical Research: Space Physics*, 111(A12). doi: <https://doi.org/10.1029/2006JA011923>
- Buneman, O. (1963, Apr). Excitation of field aligned sound waves by electron streams. *Phys. Rev. Lett.*, 10, 285–287. Retrieved from <https://link.aps.org/doi/10.1103/PhysRevLett.10.285> doi: 10.1103/PhysRevLett.10.285
- Burrell, A., van der Meeren, C., & Laundal, K. M. (2020, January). *aburrell/aacgmv2: Version 2.6.0*. Zenodo. Retrieved from <https://doi.org/10.5281/zenodo.3598705> doi: 10.5281/zenodo.3598705
- Chau, J. L., & St.-Maurice, J. (2016). Unusual 5 m E region field-aligned irregularities observed from northern Germany during the magnetic storm of 17 March 2015. *Journal of Geophysical Research: Space Physics*, 121(10), 10,316–10,340. Retrieved from <https://agupubs.onlinelibrary.wiley.com/doi/abs/10.1002/2016JA023104> doi: 10.1002/2016JA023104
- Chen, X.-C., Lorentzen, D. A., Moen, J. I., Oksavik, K., & Baddeley, L. J. (2015). Simultaneous ground-based optical and HF radar observations of the ionospheric foot-

- print of the open/closed field line boundary along the geomagnetic meridian. *Journal of Geophysical Research: Space Physics*, 120(11), 9859-9874. doi: <https://doi.org/10.1002/2015JA021481>
- Chisham, G., Lester, M., Milan, S., Freeman, M., Bristow, W., Grocott, A., ... others (2007). A decade of the Super Dual Auroral Radar Network (SuperDARN): Scientific achievements, new techniques and future directions. *Surveys in geophysics*, 28(1), 33–109.
- Cogger, L., Howarth, A., Yau, A., White, A., Enno, G., Trondsen, T., ... others (2015). Fast Auroral Imager (FAI) for the e-POP mission. *Space Science Reviews*, 189(1-4), 15–25.
- Farley, D. T. (1963, Apr). Two-stream plasma instability as a source of irregularities in the ionosphere. *Phys. Rev. Lett.*, 10, 279–282. Retrieved from <https://link.aps.org/doi/10.1103/PhysRevLett.10.279> doi: 10.1103/PhysRevLett.10.279
- Gattinger, R. L., Vallance Jones, A., Degenstein, D. A., & Llewellyn, E. J. (2010). Quantitative spectroscopy of the aurora. vi. the auroral spectrum from 275 to 815 nm observed by the OSIRIS spectrograph on board the Odin spacecraft. *Canadian Journal of Physics*, 88(8), 559-567. doi: <https://doi.org/10.1139/P10-037>
- Greenwald, R., Baker, K., Dudeney, J., Pinnock, M., Jones, T., Thomas, E., ... others (1995). Darn/SuperDARN. *Space Science Reviews*, 71(1-4), 761–796.
- Hosokawa, K., Motoba, T., Yukimatu, A. S., Milan, S. E., Lester, M., Kadokura, A., ... Bjornsson, G. (2010). Plasma irregularities adjacent to auroral patches in the postmidnight sector. *Journal of Geophysical Research: Space Physics*, 115(A9). doi: <https://doi.org/10.1029/2010JA015319>
- Huyghebaert, D., Hussey, G., Vierinen, J., McWilliams, K., & St-Maurice, J.-P. (2019). ICEBEAR: An all-digital bistatic coded continuous-wave radar for studies of the E region of the ionosphere. *Radio Science*, 54(4), 349-364. Retrieved from <https://agupubs.onlinelibrary.wiley.com/doi/abs/10.1029/2018RS006747> doi: 10.1029/2018RS006747
- Huyghebaert, D., McWilliams, K., Hussey, G., Galeschuk, D., Chau, J. L., & Vierinen, J. (2021). Determination of the azimuthal extent of coherent E-region scatter using the ICEBEAR linear receiver array. *Radio Science*, 56(3), e2020RS007191. doi: <https://doi.org/10.1029/2020RS007191>
- Hysell, D. (2018). *Antennas and radar for environmental scientists and engineers*. Cambridge University Press. doi: 10.1017/9781108164122
- Hysell, D., Miceli, R., Munk, J., Hampton, D., Heinselman, C., Nicolls, M., ... Lessard, M. (2012). Comparing VHF coherent scatter from the radar aurora with incoherent scatter and all-sky auroral imagery. *Journal of Geophysical Research: Space Physics*, 117(A10). Retrieved from <https://agupubs.onlinelibrary.wiley.com/doi/abs/10.1029/2012JA018010> doi: 10.1029/2012JA018010

- Kelley, M. C. (2009). Instabilities and structure in the high-latitude ionosphere. In *The Earth's ionosphere* (Vol. 96, p. 469-544). Academic Press. doi: [https://doi.org/10.1016/S0074-6142\(09\)60227-8](https://doi.org/10.1016/S0074-6142(09)60227-8)
- Knudsen, D. J., Burchill, J. K., Buchert, S. C., Eriksson, A. I., Gill, R., Wahlund, J.-E., ... Moffat, B. (2017). Thermal ion imagers and langmuir probes in the Swarm electric field instruments. *Journal of Geophysical Research: Space Physics*, *122*(2), 2655-2673. Retrieved from <https://agupubs.onlinelibrary.wiley.com/doi/abs/10.1002/2016JA022571> doi: 10.1002/2016JA022571
- Lee, Y.-S., Kwak, Y.-S., Kim, K.-C., Solheim, B., Lee, R., & Lee, J. (2017). Observation of atomic oxygen O(1S) green-line emission in the summer polar upper mesosphere associated with high-energy (≥ 30 keV) electron precipitation during high-speed solar wind streams. *Journal of Geophysical Research: Space Physics*, *122*(1), 1042-1054. doi: <https://doi.org/10.1002/2016JA023413>
- Lester, M., Milan, S. E., Besser, V., & Smith, R. (2001). A case study of HF radar spectra and 630.0 nm auroral emission in the pre-midnight sector. *Annales Geophysicae*, *19*(3), 327-339. doi: <https://doi.org/10.5194/angeo-19-327-2001>
- Marklund, G. (1984). Auroral arc classification scheme based on the observed arc-associated electric field pattern. *Planetary and Space Science*, *32*(2), 193-211. doi: [https://doi.org/10.1016/0032-0633\(84\)90154-5](https://doi.org/10.1016/0032-0633(84)90154-5)
- Megan Gillies, D., Knudsen, D., Donovan, E., Jackel, B., Gillies, R., & Spanswick, E. (2017). Identifying the 630 nm auroral arc emission height: A comparison of the triangulation, FAC profile, and electron density methods. *Journal of Geophysical Research: Space Physics*, *122*(8), 8181-8197. doi: <https://doi.org/10.1002/2016JA023758>
- Milan, S., Lester, M., & Moen, J. (1997). A comparison of optical and coherent HF radar backscatter observations of a post-midnight aurora. *Annales Geophysicae*, *15*(11), 1388-1398. doi: <https://doi.org/10.1007/s00585-997-1388-0>
- Moen, J., Carlson, H. C., Milan, S. E., Shumilov, N., Lybekk, B., Sandholt, P. E., & Lester, M. (2001). On the collocation between dayside auroral activity and coherent HF radar backscatter. *Annales Geophysicae*, *18*(12), 1531-1549. doi: <https://doi.org/10.1007/s00585-001-1531-2>
- Obuchi, Y., Sakanoi, T., Yamazaki, A., Ino, T., Okano, S., Kasaba, Y., ... Takeyama, N. (2008). Initial observations of auroras by the multi-spectral auroral camera on board the Reimei satellite. *Earth, planets and space*, *60*(8), 827-835. doi: <https://doi.org/10.1186/BF03352834>
- Paxton, L. J., & Meng, C.-I. (1999). Auroral imaging and space-based optical remote sensing. *Johns Hopkins APL technical digest*, *20*(4), 556-569.
- Semeter, J., Butler, T., Heinselman, C., Nicolls, M., Kelly, J., & Hampton, D. (2009). Volumetric imaging of the auroral ionosphere: Initial results from PFISR. *Journal of Atmospheric and Solar-Terrestrial Physics*, *71*(6), 738-743. doi: <https://doi.org/10.1016/j.jastp.2008.08.014>

- Shepherd, S. G. (2014). Altitude-adjusted corrected geomagnetic coordinates: Definition and functional approximations. *Journal of Geophysical Research: Space Physics*, 119(9), 7501-7521. Retrieved from <https://agupubs.onlinelibrary.wiley.com/doi/abs/10.1002/2014JA020264> doi: 10.1002/2014JA020264
- St.-Maurice, J.-P., & Chau, J. L. (2016). A theoretical framework for the changing spectral properties of meter-scale Farley-Buneman waves between 90 and 125 km altitudes. *Journal of Geophysical Research: Space Physics*, 121(10), 10,341-10,366. Retrieved from <https://agupubs.onlinelibrary.wiley.com/doi/abs/10.1002/2016JA023105> doi: 10.1002/2016JA023105
- SuperDARN Data Analysis Working Group (DAWG), Schmidt, M., Billett, D., Martin, C., Huyghebaert, D., Bland, E., ... et al. (2021, Feb). *Superdarn/pydarn: pydarnio v2.0.1*. Zenodo. doi: 10.5281/zenodo.4558130
- SuperDARN Data Standards Working Group (DSWG), Schmidt, M., Billett, D., Bland, E., Burrell, A., Detwiller, M., ... et al. (2020, Aug). *Superdarn/pydarnio: pydarnio v1.0*. Zenodo. doi: 10.5281/zenodo.4009471
- Wahlund, J. E., Opgenoorth, H. J., Häggström, I., Winser, K. J., & Jones, G. O. L. (1992). EISCAT observations of topside ionospheric ion outflows during auroral activity: Revisited. *Journal of Geophysical Research: Space Physics*, 97(A3), 3019-3037. doi: <https://doi.org/10.1029/91JA02438>

6 Publications

6.1 Accepted Journal Publications

Huyghebaert, D., McWilliams, K., Hussey, G., Galeschuk, D., Chau, J. L., Vierinen, J. (2021). Determination of the azimuthal extent of coherent E-region scatter using the ICEBEAR linear receiver array. *Radio Science*, 56, e2020RS007191. <https://doi.org/10.1029/2020RS007191>

6.2 Journal Publications in Review Process

Olifer, L., Feltman, C., Ghaffari, R., Henderson, S., **Huyghebaert, D.**, Burchill, J., Jaynes, A.N., Knudsen, D., McWilliams, K., Moen, J.I., Spicher, A., Wu, J., (2021). Swarm Observations of Dawn/Dusk Asymmetries Between Pedersen Conductance in Upward and Downward Field-Aligned Current Regions. Submitted to *Earth and Space Science*

6.3 Software Publications and Releases

SuperDARN Data Analysis Working Group, Schmidt, M.T., Billett, D.D., Martin, C.J., **Huyghebaert, D.**, Bland, E.C., Burrell, A.G., Detwiller, M.H., Herlingshaw, K., Krieger,

K., Peters, D.G.O., Reimer, A.S., Reistad, J.P., Roberston, C.R., Sterne, K.T. (2021, February 18). SuperDARN/pydarn: pyDARN v2.0 (Version v2.0). Zenodo. <http://doi.org/10.5281/zenodo.4549096>

6.4 Conferences and Workshops

SuperDARN Workshop, May 24-28, 2021, Online

Huyghebaert, D., McWilliams, K., Hussey, G., St.-Maurice, J.-P., Howarth, A., Erion, S., Rutledge, P. (2021), Comparisons Between E-region Coherent Scatter and Swarm-E Fast Auroral Imager Measurements

EGU General Assembly 2021, April 19-30, 2021, Online

Huyghebaert, D., McWilliams, K., Hussey, G., Howarth, A., Erion, S., Rutledge, P. (2021), Comparisons Between E-region Coherent Scatter and Swarm-E Fast Auroral Imager Measurements

DASP Meeting 2021, February 15-19, 2021, Online

Huyghebaert, D., McWilliams, K., Hussey, G., Howarth, A., Erion, S., Rutledge, P. (2021), Comparisons Between E-region Coherent Scatter and Swarm-E Fast Auroral Imager Measurements

Living Planet Fellowship Annual Workshop, December 3, 2020, Online

Huyghebaert, D. (2020), A Swarm, SuperDARN, and ICEBEAR Collaboration – Turbulent E-region Aurora Measurements

AGU Fall Meeting 2020, December 1-17, 2020, Online

Huyghebaert, D., McWilliams, K., Hussey, G., Galeschuk, D., Chau, J.L., and Vierinen, J. (2020), Results from Mapping ICEBEAR Coherent E-region Scatter Using a Linear Receiving Array

SuperDARN Workshop, June 1-5, 2020, Online

Huyghebaert, D., Hussey, G.C., McWilliams, K.A., Galeschuk, D., Chau, J.L. and Vierinen, J.P. (2020), Determination of the Azimuthal Extent of Coherent E-region Scatter Using the ICEBEAR Linear Receiver Array

EGU General Assembly 2020, May 4-8, 2020, Online

Huyghebaert, D., Lozinsky, A., Hussey, G.C., McWilliams, K.A., Galeschuk, D., St.-Maurice, J.P., Urco, J.M., Chau, J.L. and Vierinen, J.P. (2020), ICEBEAR: Recent Results from a Bistatic Coded Continuous-Wave E-region Coherent Scatter Radar